water

MDPI

Article

Differentiated Effects of Urbanization on Precipitation in South China

Lingli Fan [1], Guangya Zhang [2,*] and Jianjun Xu [1]

[1] College of Ocean and Meteorology, South China Sea Institute of Marine Meteorology, Guangdong Ocean University, Zhanjiang 524088, China; fanll@gdou.edu.cn (L.F.); gmuxujj@163.com (J.X.)
[2] Education Information Center, Guangdong Ocean University, Zhanjiang 524088, China
* Correspondence: zhanggy@gdou.edu.cn; Tel.: +86-759-296-6993

Abstract: In this paper, precipitation data from the Tropical Rainfall Measuring Mission (TRMM), together with atmospheric reanalysis data, are employed to identify warm-season precipitation (1998–2014) changes and their association with rapid urbanization in south China. Three urban clusters (Chenyu, Yangtze Delta, and Fujian Guangdong coast) are focused. The results reveal that, for the inland Chengyu urban cluster, a lack of precipitation trend is likely due to insignificant trends in convective available potential energy (CAPE) and total column water vapor (TCWV). They are likely resulted from a reduced local moisture recycling in urban areas, balanced by an increased evapotranspiration of rural areas, together with a stable advection of water vapor input. For the Yangtze River Delta urban cluster, a negative trend in precipitation is associated with a slightly decreased CAPE and an increased TCWV, but is very likely related to urbanization induced an increased planetary boundary layer (PBL) and reduced land surface evaporation. For the Fujian Guangdong coast urban cluster, a marked positive precipitation trend is well explained by positive trends in CAPE and TCWV. The increased precipitation likely benefits from enhanced moisture recycling due to improved vegetation cover in rural areas, and enhanced advection moisture inputs due to urbanization along the coast. These results suggest urbanization effects on precipitation vary with regional conditions. In the coastal area, urbanization enhances sea breezes, which may benefit precipitation if sea breezes go along with the prevailing moisture. In inland area, urbanization likely leads to a warmer-dryer climate if large-scale land cover keeps stationary.

Keywords: urbanization; warm season precipitation; regional differentiation; south China

Citation: Fan, L.; Zhang, G.; Xu, J. Differentiated Effects of Urbanization on Precipitation in South China. *Water* **2021**, *13*, 1386. https://doi.org/10.3390/w13101386

Academic Editor: David Dunkerley

Received: 22 April 2021
Accepted: 14 May 2021
Published: 16 May 2021

1. Introduction

At present, 55% of the world's population resides in urban areas. The urban population is expected to reach 68% by 2050 (the Population Division of the UN DESA, 2018). Urbanization's effect on precipitation has been recognized for four decades [1–3]. Such effects are receiving increasing attention because they may exacerbate torrential rain, which threatens urban societies [4]. Previous studies suggest that urban-induced changes in precipitation processes most likely result from one or more of the following five mechanisms [5–10] : (1) atmospheric destabilization through influences of mesoscale circulation, (2) increased low-level convergence due to surface roughness, (3) modification of microphysical and dynamic processes by the addition of aerosols, (4) modification of low-level atmospheric moisture content, and (5) large structures create a bifurcation zone that steers storms around cities. These mechanisms potentially have either positive or negative effects on precipitation processes depending on the available moisture in the environment.

Numerous investigations of urbanization impact on precipitation are based on statistical analysis of rain gauge networks [11–13], ground-based radar [14–16], or model

simulations [17–21]. Some authors have applied remote-sensing data (Tropical Rainfall Measuring Mission precipitation data, TRMM) to identify patterns in warm-season precipitation anomalies around cities [22–31]. Although useful, these studies are limited to specific cities with special observation networks, theoretical model simulations, or mainly focused on representative events.

Many previous studies have shown that urbanization leads to increased precipitation during the warm-season months. It was shown that the areal extent and magnitude of downwind precipitation anomalies are related to the sizes of the urban area [1,32–39]. Numerical model simulations are consistent with the anomalies found from observational studies [40–44].

However, some other studies have shown that the urbanization effect is negligible in precipitation formation [41,45,46]. A negative urbanization effect on precipitation has been reported in some studies [47–52]. In one study, this effect has been attributed to urban-induced changes in regional surface hydrology [51]. These different conclusions suggest that the urbanization effects on precipitation may vary with local climate settings and land cover conditions.

Thus, further studies are necessary to quantify the urban effect on precipitation over urban clusters located in different geographic and climatic conditions around the world. South China is one area with rapid urbanization in the last two decades. Simultaneously, vegetation cover in the rural areas has significantly changed [53–58]. In this study we aim to investigate the possible impacts of rapid urbanization on precipitation in South China. The research questions are (1) whether warm season precipitation in South China has experienced observable changes in recent decades; and (2) whether these precipitation trends (if exist) are associated with urbanization.

It is necessary to briefly introduce the studied region. The region covers most of South China (100.0–125.5° E, 18.5–35.0° N) urban clusters (Figure 1a). The main moisture sources in warm season of this region and its surroundings are the South China Sea, the Bay of Bengal, and the western Pacific Ocean [58–60].

The study region covers most of South China, which has experienced rapid development since early 1990s. Three urban clusters are representative for the urbanization in the recent decades in China. The Chengyu urban cluster (Figure 1b) is located in the southwest of China, the red rectangle marks it in Figure 1a. The landform features rugged mountains and valleys. It has a subtropical monsoon humid climate, with a hot summer and a warm winter. The mean annual precipitation is about 1200 mm. Precipitation primarily occurs from June to August, accounting for 70% of the annual precipitation.

The Yangtze River Delta urban cluster (Figure 1c) is located in the coast of the East China Sea, the orange rectangle marks it in Figure 1a. The landform mainly features a low and flat plain with relatively high density of surface water bodies. It is significantly influenced by humid subtropical monsoon circulation, with a mean annual precipitation of about 1100 mm. Summer is the main rainy season [61].

The Pearl River Delta urban cluster and the West Coast of the Taiwan Strait urban cluster (Figure 1d, in this paper, it is called the Fujian Guangdong coast urban cluster) are located in the southeastern coast of China; the blue rectangle marks it in Figure 1a. The landform mainly features a middle and low mountains-delta plain. It has a typical marine subtropical monsoon climate. It receives on average about 1000–2000 mm of precipitation per year. Most of it occurs in warm season (April–September).

According to the climate change regionalization in China (1961–2010) [62], the Chengyu cluster belongs to the Southwest China–South China dry-warm trend zone, the Yangtze River Delta urban cluster is part of the East China–Central China wet-warm trend zone, the Fujian Guangdong coast cluster belongs to the East China–Central China wet-warm trend zone too.

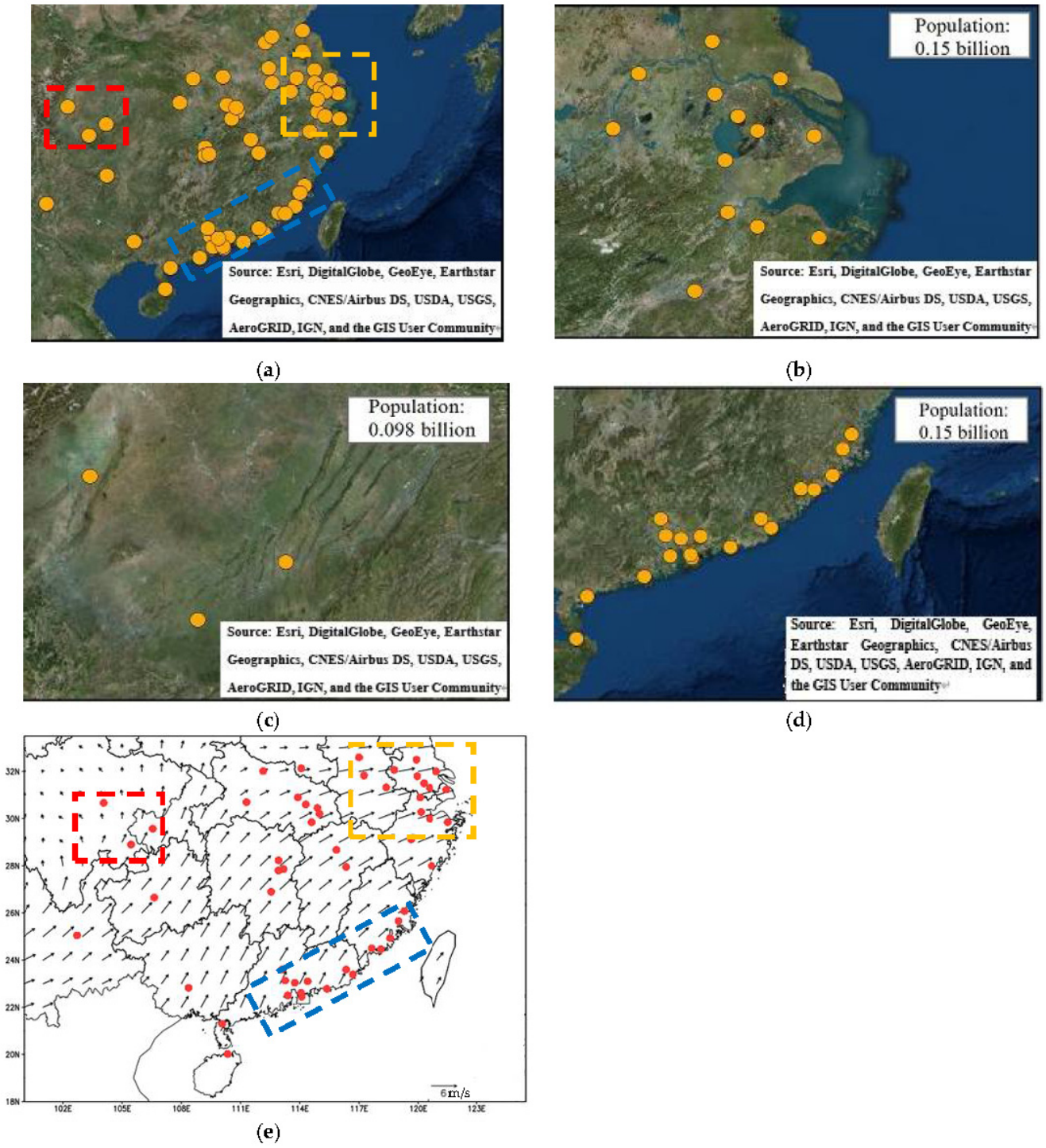

Figure 1. Distribution of cities with population over one million in 2016: (**a**) South China, (**b**) the Chengyu, (**c**) the Yangtze River Delta, and (**d**) Fujian Guangdong coast urban cluster. (**e**) Mean 700 hPa horizontal wind ($m \cdot s^{-1}$, May–September) based on ECMWF reanalysis dataset from 1998 to 2014. The solid dots indicate the cities with population over one million in 2016.

As the urban effects on precipitation appear to be different between upwind and downwind to the urban area [8,42,63], the mean May–September 700 hPa horizontal wind during 1998–2014 (the study period) is analyzed, summarized in Figure 1e. The 700 hPa level is chosen as the representative level for the mean steering flow, following previous studies [64]. Southwesterly winds prevail in the South China during the warm-season, which is associated with the East Asian summer monsoon system.

The urban effects are most pronounced during warm-season months [37,63,65]. Warm-season precipitation over China is significantly correlated with the convergence of the water vapor transport and deep convections [66–68]. During the warm season, the urbanization-induced mesoscale circulation is more prominent and can significantly alter boundary layer processes. Thus, the present study focuses on the warm-season months (May–September) of 1998–2014, because the available TRMM rain data just cover a period of 1998–2014.

2. Materials and Methods

2.1. Data

Monthly atmospheric datasets, including convective available potential energy (CAPE), total column water vapor (TCWV), are obtained from the European Centre for Medium-Range Weather Forecasts (ECMWF, https://apps.ecmwf.int/datasets/data/interim-full-moda/levtype=sfc/, accessed on 20 February 2019). The data have a resolution of 0.125° *0.125° (about 12.5 km), and cover a period of 1979–2019 [69]. Data of hourly surface rain rate (unit: mm·h-1) are obtained from the TRMM 3G68 (hereafter referred to as PR 3G68) dataset, provided by GSFC/NASA (Goddard Space Flight Center, National Aeronautics and Space Administration, ftp://trmmopen.gsfc.nasa.gov/pub, accessed on 20 February 2019). It is a gridded product that combines the TRMM satellite Precipitation Radar (PR), TRMM Microwave Imager (TMI) and TRMM combined instrument at 0. 5°*0. 5° (about 50 km) and hourly resolution, 1998–2014. The rainfall rate also includes total rainfall from each instrument and convective rainfall and convective fraction. Because the data are gridded hourly and put in a daily file, there are a lot of hours with missing data due to satellite sampling, the percent of sampling error are higher for low rain rate than high rain rate [70–72]. The GIMMS 3g NDVI v1 dataset provided by ECOCAST (NASA Ames Ecological Forecasting Lab, https://ecocast.arc.nasa.gov/data/pub/gimms/, accessed on 20 February 2019), at 1/12° × 1/12° and 15-days resolution, 1981–2015.

2.2. Methods

Although the TRMM dataset is not sufficient to establish true climatological behavior, the 17-year period, overlapped with the rapid urbanization in South China, allows for the investigation of anomalies in precipitation associated with urban effects. The analysis is primarily conducted based on hourly precipitation rates ($mm \cdot h^{-1}$) in 0.5° × 0.5° cells.

For more detailed analysis, mean surface precipitation rates at each grid point are calculated for the months of May, June, July, August, and September. For a given grid cell, hourly surface precipitation rates are averaged for the five warm-season months. This average hourly rain rate is multiplied by (24 h × 30/31 days × 5 months) to obtain the warm-season precipitation of the grid cell for the year. This procedure is repeated for each of the 17 years, resulting in a 17-year time series of warm season precipitation for 1998–2014.

The possible relationship between precipitation trend and urbanization in South China is analyzed as follows. Firstly, the 17-year warm season precipitation is examined for trends. Secondly, the variability of atmospheric parameters is examined to explain the precipitation trends (if there are). Thirdly, possible connections between these mechanisms and the urbanization are examined.

3. Results

3.1. Interannual Variation of Warm Season Precipitation in South China

No obvious pattern of any trend of the spatially average warm-season precipitation occurs over South China during 1998–2014, while the population density and urban built-up area, represented by the selected cities increase rapidly (Table 1). Nevertheless, the precipitation trends are observed in subregions. The maximum trend of warm-season precipitation (3–6 $mm \cdot mon^{-1} \cdot year^{-1}$, Figure 2a) distributes in the downwind and surrounding areas of the Fujian Guangdong coast cluster (Figure 1e). This confirms previous research

result: an increasing trend of precipitation existed at the Pearl River Delta [12,13]. Warm-season rainfall decreases over the Chengyu urbanized areas (Figure 2a, −3 mm·mon^{-1}·year^{-1}) and increases slightly in its downwind areas (Figure 2a, 0–3 mm·mon^{-1}·year^{-1}). Precipitation decreases over the Yangtze River Delta urban cluster (Figure 2a, −3 mm·mon^{-1}·year^{-1}). Both convective (Figure 2b, 0–6 mm·mon^{-1}·year^{-1}) and non-convective precipitation (Figure 2c, 3–9 mm·mon^{-1}·year^{-1}) increases in the area associated with the Fujian Guangdong coast urban cluster. The convective rain (Figure 2b, −3–3 mm·mon^{-1}·year^{-1}) appears to be stable, while non-convective rain (Figure 2c, −6–0 mm·mon^{-1}·year^{-1}) decreases over the Chengyu urbanization area. For the downwind rural area, both convective (Figure 2b, 0–3 mm·mon^{-1}·year^{-1}) and no-convective precipitation (Figure 2c, 3–6 mm·mon^{-1}·year^{-1}) increase slightly. Both convective (Figure 2b, −3 mm·mon^{-1}·year^{-1}) and non-convective precipitation (Figure 2c, −6–−3 mm·mon^{-1}·year^{-1}) decreases over the Yangtze River Delta urban cluster.

Table 1. Linear regression between the relevant factors and Year.

Factors	The Linear Fitting Equation
Warm-season rainfall (mm·mon^{-1})	$y = -0.33t + 142.0$
Building completed area (10^6 m^2)	$y = 401.83t + 2013.1$
Urban population of selected cities (10^4 persons)	$y = 133.94t + 10021.0$

The convective precipitation percentage (CPP) slightly increases in the Fujian Guangdong coast cluster (Figure 2d, 0.1–0.3%·year^{-1}). The increase of CPP over the Chengyu urbanization area (Figure 2d, 0.3–0.5%·year^{-1}) is more evident than its rural area (Figure 2d, 0.1–0.2%·year^{-1}). The CPP shows a decreasing trend over the Yangtze River Delta urban cluster (Figure 2d, −0.2%·year^{-1}). Nevertheless, warm season convective and non-convective precipitation appears to have similar trends during the study period (Figure 2b,c, Table 2).

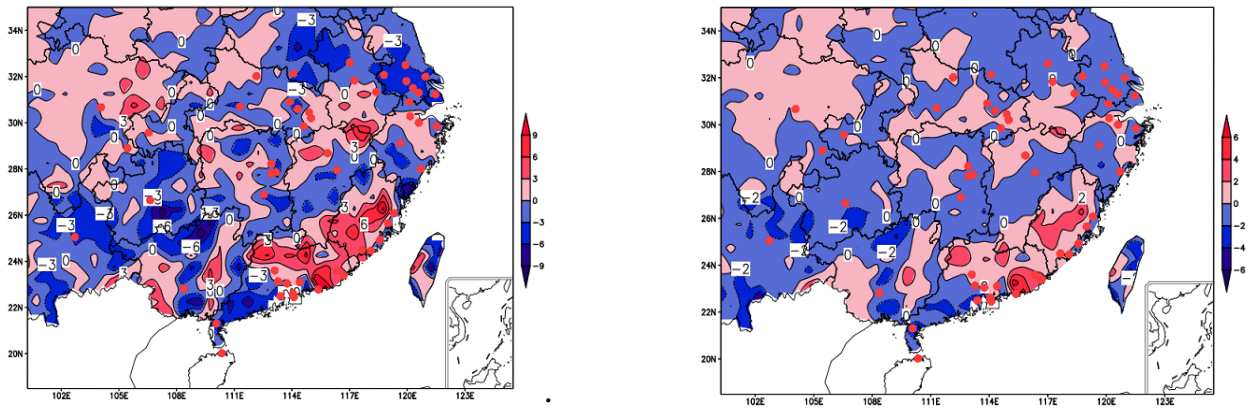

(**a**) (**b**)

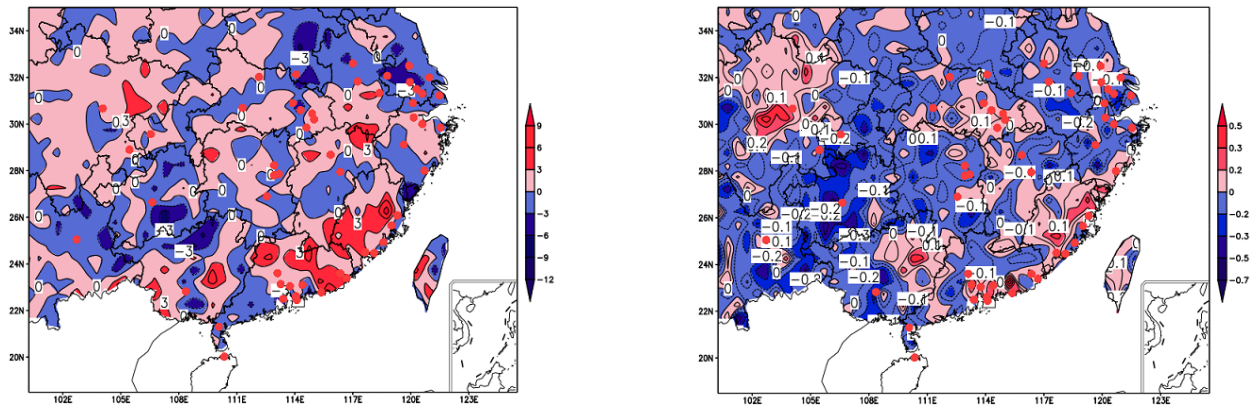

(**c**) (**d**)

Figure 2. Contour plots of the 17-year (1998–2014) trends over South China: (**a**) warm-season (May–September) precipitation (mm·mon^{-1}·year^{-1}), (**b**) convective precipitation (mm·mon^{-1}·year^{-1}), (**c**) non-convective precipitation (mm·mon^{-1}·year^{-1}), (**d**) convective precipitation percentage (%·year^{-1}), based on 0.5°*0.5° TRMM PR rain rate data.

Table 2. The trend of rain, CAPE, TCWV, skin-temperature, sensible heat flux, boundary layer height, evaporation, 1000 hPa specific humidity in warm season during 1998 to 2014.

Urban Clusters.	Chenyu	The Yangtze River Delta	Fujian Guangdong Coast
Rain trend (mm·mon^{-1}·year^{-1})	−3–6	−6–−3	3–6
convective precipitation (mm·mon^{-1}·year^{-1})	−2–2	−2–0	0–4
non-convective precipitation (mm·mon^{-1}·year^{-1})	−3–3	−6–0	0–6
CAPE (J·kg^{-1}·year^{-1})	−5–5	−5–5	5–10
TCWV (kg·m^{-2}·year^{-1})	−0.05–0.05	0.05–0.1	0.05–0.1
Skin-temperature (°C·year^{-1})	0–0.12	0.03	0.03
Sensible heat flux (W·m^{-2}·year^{-1})	0–1.0	0.2–0.4	0–0.2
Boundary layer height (m·year^{-1})	0–18	2–4	−2
Evaporation (Kg·m^{-2}·s·year^{-1})	−1–2	−1	1–2
1000 hPa specific humidity (kg·kg^{-1}·year^{-1})	−3–2	2	2

3.2. Association of Spatially Differentiated Trends in Precipitation and Two Atmospheric Variables Surrounding the Three Urban Clusters

Precipitation is a product of condensation of the atmospheric water vapor, in which the atmospheric instability and convection play a significant role. The CAPE is a good indicator for atmospheric instability and convection [30,51]. Previous studies have shown a tight relationship between precipitation and TCWV as well [68,73]. To examine the associated physical mechanisms leading to the precipitation trends observed in surrounding the three urban clusters, variations in CAPE and TCWV are first examined.

The spatially distributed CAPE and TCWV trends are shown in Figure 3 and Table 2 The overall northeast-southwest oriented zone of both negative CAPE and TCWV trends explain the slightly negative trend of warm season precipitation in these areas of South China (Figure 2). The area with both positive CAPE (Figure 3a, 5~10 J·kg^{-1}·year^{-1}) and TCWV (Figure 3b, 0.05~0.1 kg·m^{-2}·year^{-1}) trends coincidently delineates the upward trend of warm season precipitation downwind from the Fujian Guangdong coast urban cluster.

For Chengyu urban cluster, no marked trend in precipitation is likely because the insignificant trends in CAPE (Figure 3a, −5~5 J·kg^{-1}·year^{-1}) and TCWV (Figure 3b, −0.05~0.05 kg·m^{-2}·year^{-1}). For Yangtze River Delta urban cluster, negative trend in precipitation, which is not explained well by a slightly negative CAPE trend (Figure 3a, −5~5 J·kg^{-1}·year^{-1}) but slightly positive TCWV trend (Figure 3b, 0.05~0.1 kg·m^{-2}·year^{-1}).

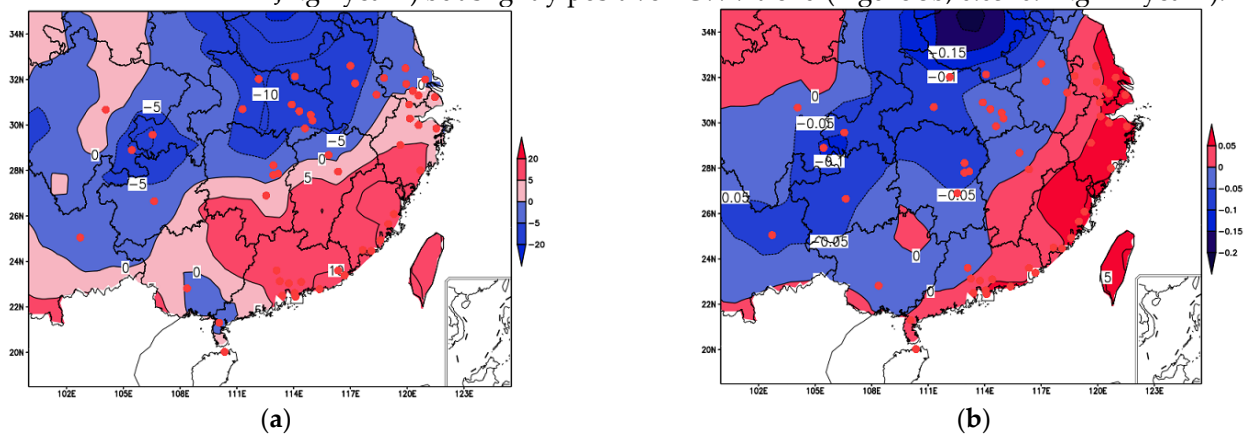

Figure 3. A contour plot of the 17-year, warm-season trend using 0.125° × 0.125° ECMWF data: (**a**) CAPE (J·kg^{-1}·year^{-1}), (**b**) total column water vapor (kg·m^{-2}·year^{-1}).

3.3. Possible Mechanisms

From Section 3.2, it seems that the overall the spatially differentiated warm season precipitation trends in South China are associated with the trends in CAPE and TCWV. Whether and how the urbanization in South China has contributed to these trends remain to be seen. If urbanization has an influence, it must realize through modifying the surface and low atmosphere conditions. Figure 4 and Table 2 show the changes in the surface and lower atmosphere during warm-season of 1998–2014 in South China. The urbanization effects on skin temperature are clear. The maximum trend value of warm-season skin-temperature is 0.12 °C·year^{-1} (Figure 4a), occurs in Chengyu urbanized areas. The trend of the Yangtze River Delta urban cluster and the Fujian Guangdong coast urban cluster are around 0.03 °C·year^{-1}, which is close to the results of previous studies based on model simulation [20,21]. Our research, based on remote-sensing data, classify and discuss the possible mechanisms of urban effect on precipitation under different geographic and climatic conditions.

3.3.1. Possible Mechanisms for Stationary Warm Season Precipitation in the Chengyu Urban Cluster

Over and upwind of Chengyu urbanized areas, there are significant trends of skin-temperature (0.12 °C·year^{-1}, Figure 4a), sensible heat flux (0.4–1.0 W·m^{-2}·year^{-1}, Figure 4b) and PBL height (2–18 m·year^{-1}, Figure 4c), decreased evaporation (−1 × 10^{-7} Kg·m^{-2}·s·year^{-1}, Figure 4d), decreased 1000 hPa specific humidity (Figure 4e, −3 × 10^{-5} kg·kg^{-1}), and CAPE (Figure 3a, −5 J·kg^{-1}·year^{-1}). In the downwind of Chengyu urban cluster, the trends of skin-temperature (0–0.06 °C·year^{-1}, Figure 4a), sensible heat flux (0–0.4 W·m^{-2}·year^{-1}, Figure 4b) and PBL height (0–2 m·year^{-1}, Figure 4c) are insignificant, with a slightly increased evaporation (0–2 × 10^{-7} Kg·m^{-2}·s·year^{-1}, Figure 4d), 1000 hPa specific humidity (Figure 4e, 0–2 × 10^{-5} kg·kg^{-1}), and an insignificant trend in CAPE (Figure 3a, −5~5 J·kg^{-1}·year^{-1}). For this urban cluster, urban precipitation has decreased slightly, while the rural areas experienced a small increasing precipitation. During the same period, no significant change in large-scale advection of water vapor input has occurred to the region (Figure 4f). These can be explained by, in the marked urban areas, the decreased annual maximum Normalized Difference Vegetation Index (NDVI, Figure 5, −50–0 index·year^{-1}) leads an enhanced skin-temperature, an increased sensible heat flux and a higher PBL, and hence the water vapor to be mixed more evenly in a larger thickness in the lower

atmosphere. The decreased evaporation associated with a higher PBL leads to a decreased 1000 hPa specific humidity, which reduces latent heat release with air masses upward motion. Reduced local moisture recycling in the urban cluster, contributes to reducing CAPE. For the rural areas downwind from this urban cluster, local moisture recycling increases (including evaporation and TCWV) likely associated with improved vegetation cover in the rural China in recent decades [29,54,56], an increased trend of annual maximum NDVI in this rural area (Figure 5, 50–100 ndvi·year^{-1}). Thus, the overall insignificant precipitation trend over this urban cluster and its downwind area is likely supported by little change in large-scale circulation (Figure 4f), and the offset between reduced urban moisture recycling and increased rural evapotranspiration.

3.3.2. Possible Mechanisms Leading to Decreased Precipitation in the Yangtze River Delta Urban Cluster

Over the Yangtze River Delta urban cluster, the results indicate an increased skin-temperature (around 0.03 °C·year^{-1}, Figure 4a), sensible heat flux (0.2–0.4 W·m^{-2}·year^{-1}, Figure 4b), and a PBL height (2–4 m·year^{-1}, Figure 4c). They together explain a slightly decreased CAPE. An increased TCWV is supported by an increased 1000 hPa specific humidity (2 × 10^{-5} kg·kg^{-1}, Figure 4e), but not by a decreased evaporation (around −1 × 10^{-7} Kg·m^{-2}·s·year^{-1}, Figure 4d).

The negative trend in precipitation, is not explained well by a slightly decreased CAPE and increased TCWV. Nevertheless, it is consistent with an increased PBL, reduced land surface evaporation. The reduced local moisture recycling is associated with urbanization in this area, reduced annual maximum NDVI (Figure 5, −50–0 ndvi·year^{-1}), this is consistent with the result of the cited literature [57]. In addition, the urbanization has led to a slightly increased land-sea 1000–925 hPa average temperature difference (−0.01–0.01 °C·year^{-1} over sea and 0.01–0.02 °C·year^{-1} over land, Figure 6), which likely has enhanced sea breezes in the daytime. However, the sea breezes may go against synoptic prevailing moisture direction. Their impact on precipitation is not clear. Thus, very likely the observed negative precipitation trend in the Yangtze River Delta is mostly likely associated with urbanization induced an increased PBL, and a reduced land surface evaporation.

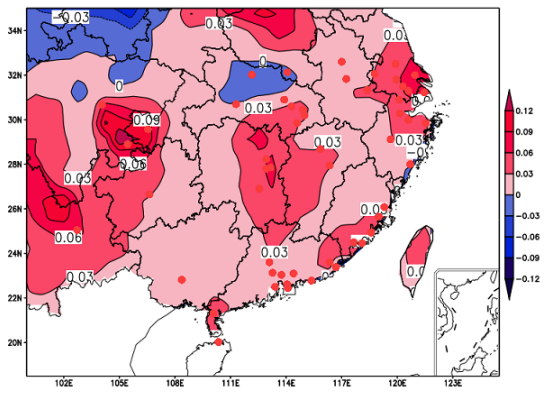

(**a**)

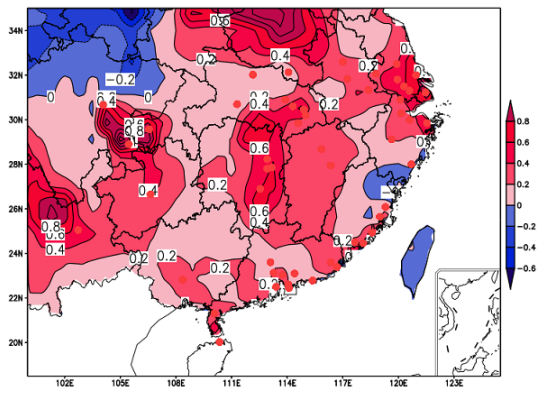

(**b**)

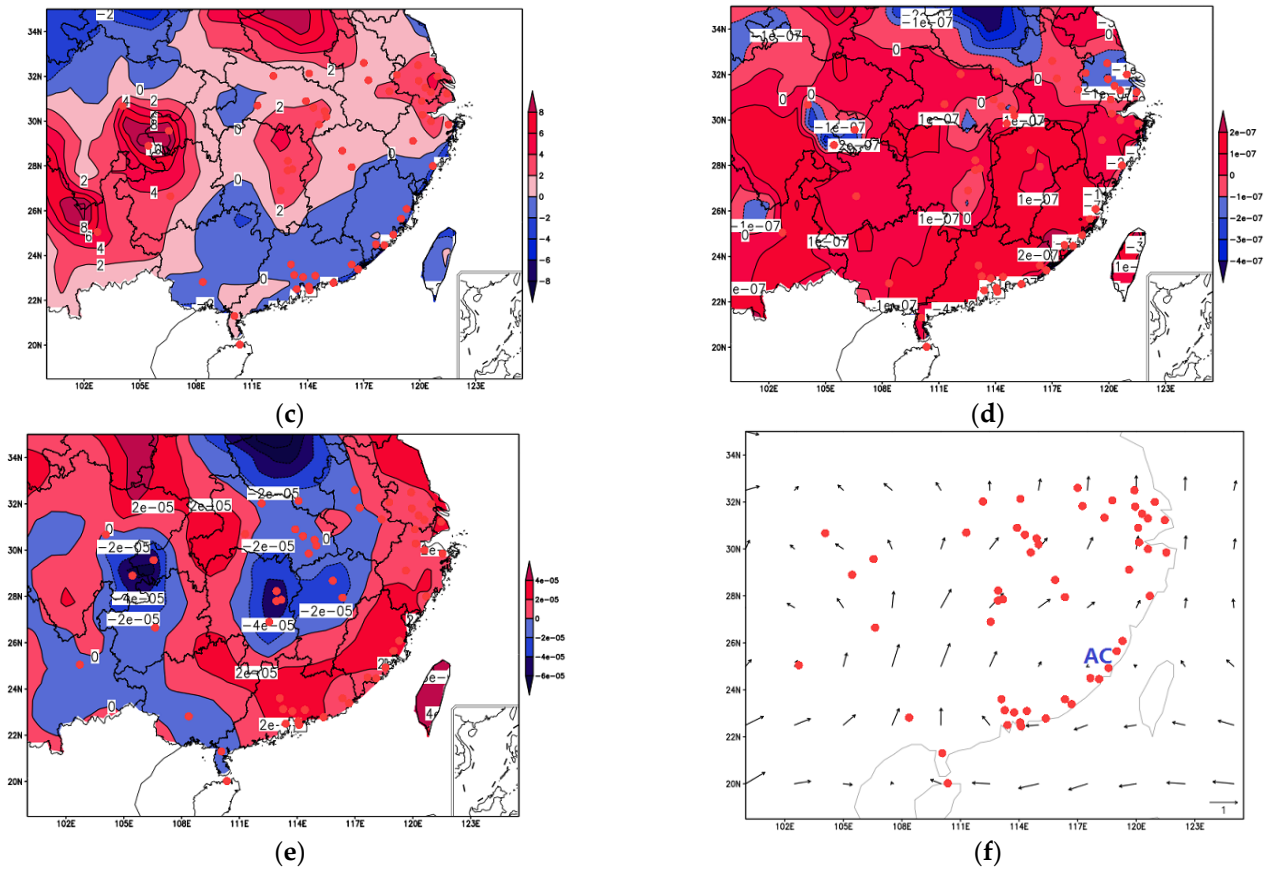

Figure 4. A contour plot of the 17-year (1998-2014), warm-season (May–September) trend of (**a**) skin-temperature(°C·year^{-1}), (**b**) sensible heat flux (W·m^{-2}·year^{-1}), (**c**) boundary layer height (m·year^{-1}), (**d**) evaporation (Kg·m^{-2}·s·year^{-1}), (**e**) 1000 hPa specific humidity (kg·kg^{-1}·year^{-1}) using 0.125° × 0.125° ECMWF data in South China. (**f**) Horizontal wind anomaly at 850 hPa during warm-season (MJJAS) 2006–2014 as the deviation from MJJAS of 1998–2005 (vectors; units: m·s^{-1}, AC indicates anticyclonic anomaly).

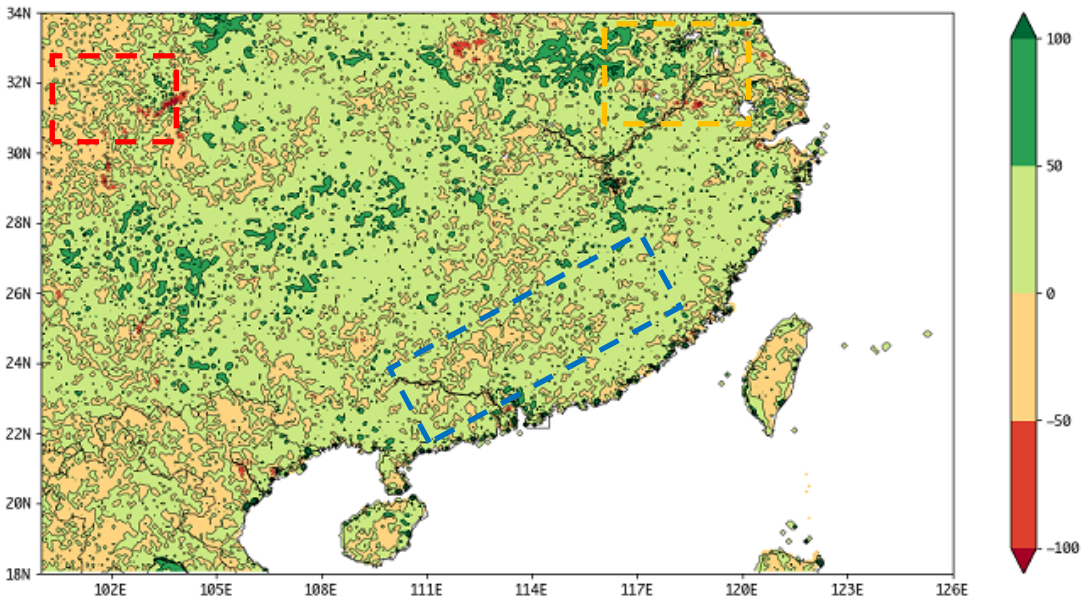

Figure 5. Trends of annual maximum NDVI over the period 1998–2014 (ndvi·year^{-1}).

3.3.3. Possible Mechanisms for an Increased Precipitation Trend in the Fujian Guangdong Coast Urban Cluster

For Fujian Guangdong coast urban cluster, consistent trends have occurred in the study period, including slightly increased skin-temperature (0.03 °C·year^{-1}, Figure 4a), sensible heat flux (0.0–0.2 W·m^{-2}·year^{-1}, Figure 4b), surface evaporation (1–2 × 10^{-7} Kg·m^{-2}·s·year^{-1}, Figure 4d) and 1000 hPa specific humidity (Figure 4e, 2 × 10^{-5} kg·kg^{-1}), while a decreased PBL height (−2 m·year^{-1}, Figure 4c). A decreased PBL height and an increased surface evaporation, contributes to a positive trend in CAPE and TCWV. They together explain the observed increased precipitation in the study period.

The reduced PBL and increased local moisture inputs are unlikely related to urbanization, but more likely associated with an improved annual maximum NDVI (Figure 5, 0–50 ndvi·year^{-1}), vegetation cover improved in this region [53,55,57]. Local positive feedback provides a favorable moisture environment. Nevertheless, the urbanization leads to an increased land-sea 1000–925 hPa average temperature gradient (0.01–0.02 °C·year^{-1} over sea and 0.03–0.04 °C·year^{-1} over land, Figure 6) [74], enhancing sea breezes. The direction of sea breezes in this region, partly along with the prevailing wind (Figure 4f), likely increases advective moisture input to the area.

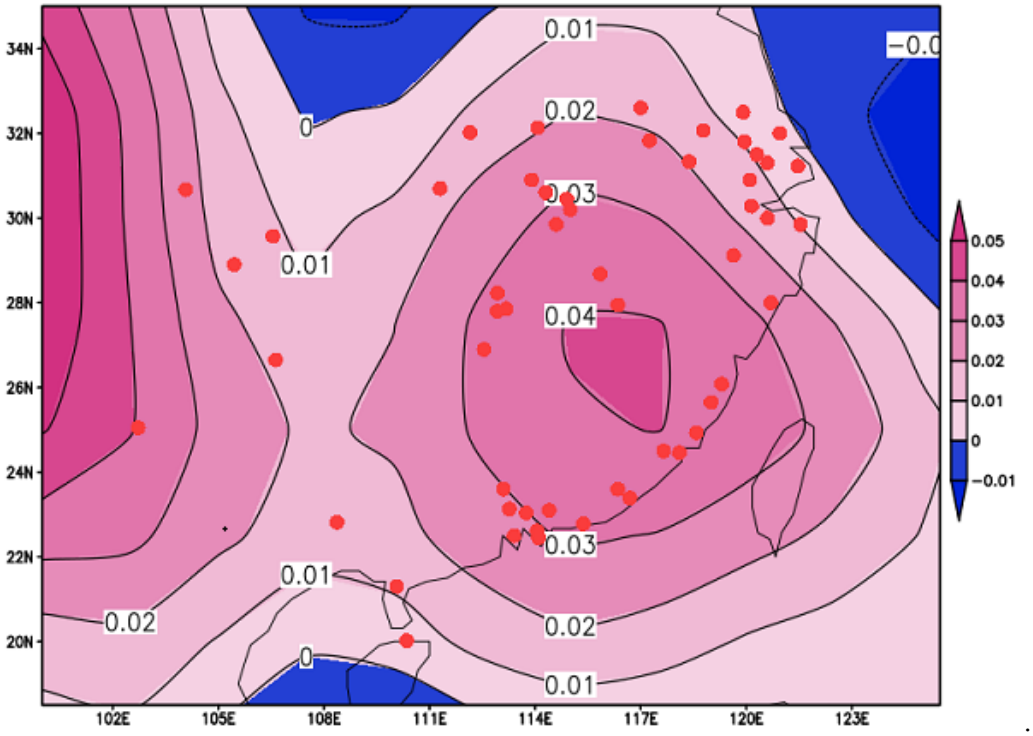

Figure 6. A contour plot of the 17-year (1998–2014), warm-season (May–September) trend of 1000–925 hPa average temperature(°C·year^{-1}).

Thus, the increased precipitation in this urban cluster is likely benefitted from enhanced moisture recycling due to an improved vegetation cover in the rural areas, and enhanced adjective moisture inputs due to urbanization along the coast.

4. Discussion

Based on the above discussion, we conceptualize the possible mechanisms for different precipitation trends at the three urban clusters (Figure 7).

In the Chenyu cluster, the urbanization has led to a reduced moisture recycling and an elevated PBL. Both tend to reduce CAPE and TCWV. These effects, however, are offset by increasing moisture recycling in the mountainous rural areas where vegetation cover

have greatly improved in recent decades [29,54,56]. Thus, overall, no marked warm season precipitation trend is observed. Should there be no vegetation cover improvement in rural area, the urbanization in this inland region, would likely become warmer and dryer.

In the Yangtze River Delta cluster, urbanization has diffused into the whole area, leading to a reducing local moisture recycling, and an elevated PBL. Both contributes to a lower CAPE. Southerly anomaly of moisture input may slightly strengthen large scale moisture inputs to the region for precipitation. This enhancement may have contributed to surface specific humidity and TCWV, but this has not translated to an increased precipitation, likely limited by a slightly negative CAPE trend.

In the Fujian Guangdong coast cluster, urbanization enhanced land-sea thermal contrast has likely induced stronger sea breezes. Meanwhile, local moisture recycling is enhanced resulting from improved vegetation cover in the rural mountainous regions [53,55,57]. Both processes have resulted in positive trends in TCWV and CAPE. They together explain the positive warm season precipitation trend.

Both along the coast, the Fujian Guangdong cluster area has seen an increase precipitation, while Yangtze River Delta has a slightly decrease trend. Two differences may provide the explanation. First, the Fujian Guangdong cluster is surrounded by a large area of mountainous landscapes where vegetation cover has greatly improved in recent decades [53,55,57], enhancing local moisture recycling, while this has not occurred the flat areas surrounding Yangtze River Delta [57]. Second, the urbanization enhanced sea breezes, tend to go along with the prevailing moisture direction for the Fujian Guangdong cluster, while against the prevailing moisture direction for the Yangtze River Delta cluster.

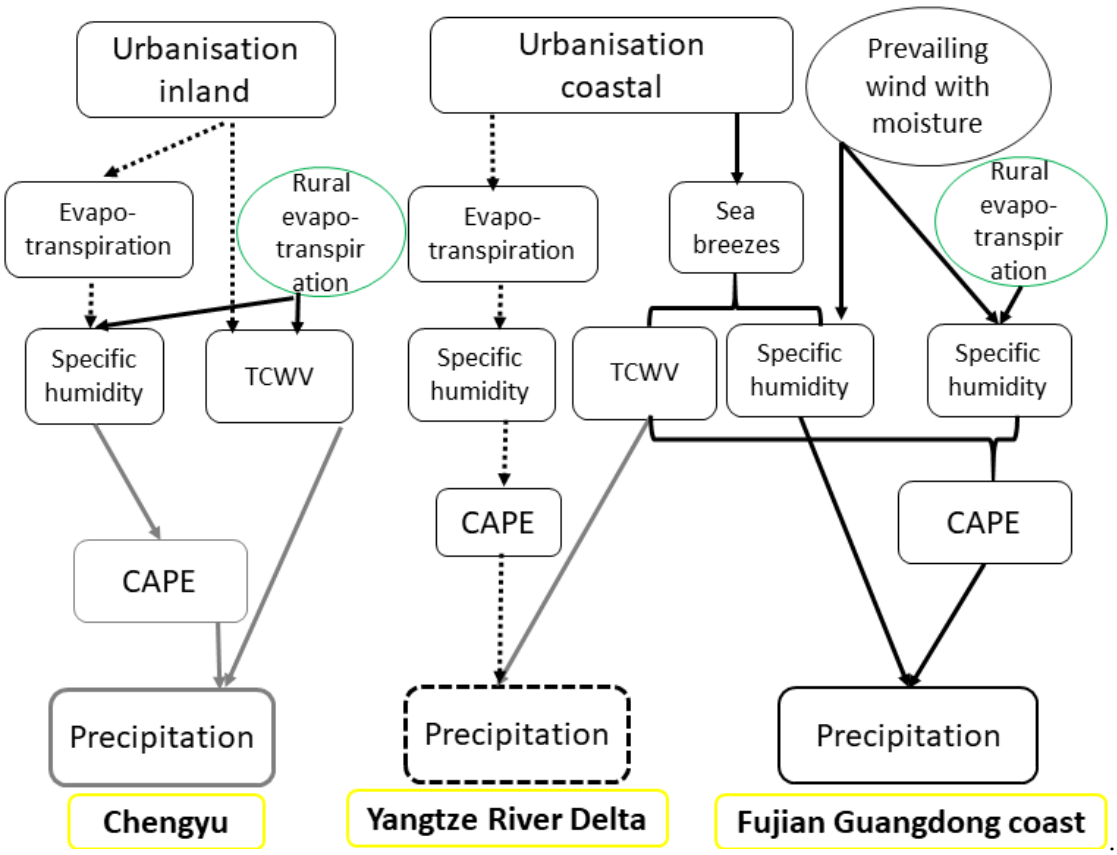

Figure 7. Conceptualization of differentiated urbanization effects on warm season precipitation in South China. The connections marked by solid lines indicate increasing with urbanization, while those marked by dot lines indicate decreasing with urbanization, those grey lines indicate negligible trend with urbanization. CAPE stands for a CAPE trend ≥ 5 ($J \cdot kg^{-1} \cdot year^{-1}$).

5. Conclusions

Using a 17-year warm season analysis of hourly rainfall rates from the TRMM 3G68 PR, we have examined the possible connections between precipitation trends and urbanization in the region of South China. Key findings are summarized as follows:

(1) There was no marked warm-season precipitation trend in Chengyu urban cluster. A downward trend of precipitation occurred over the Yangtze River Delta urban cluster. The Fujian Guangdong coast urban cluster experienced an obvious precipitation increase.

(2) For Chengyu urban cluster, a lack of precipitation trend is likely due to insignificant trends in CAPE and TCWV. These can be explained by a reduced local moisture recycling in the urban area, balanced by an increased evapotranspiration in the rural areas, together with a stable large-scale advection of water vapor input to the region.

(3) The negative trend in precipitation for the Yangtze River Delta cluster, is not explained well by a slightly decreased CAPE and increased TCWV, but seems to be associated with an increased PBL and reduced land surface evaporation. They both can be induced by rapid urbanization in this area.

(4) For the Fujian Guangdong coast urban cluster, a marked positive precipitation trend is explained by positive trends in CAPE and TCWV. The increased precipitation in this urban cluster likely benefits from enhanced moisture recycling due to improved vegetation cover in the rural areas, and enhanced adjective moisture inputs due to urbanization along the coast.

(5) In additional to urbanization, large-scale vegetation cover improvement in south China seems to have an impact on precipitation via increasing local moisture recycling. Without this vegetation cover change, an inland urbanization (e.g., Chenyu) likely makes the area warmer and dryer. In the coastal area, urbanization enhances sea breezes, which may benefit precipitation if sea breezes go along with the prevailing moisture. Therefore, in order to reduce the risk of making the area warmer and dryer, it is necessary to improve the large-scale vegetation cover in the process of urbanization.

Author Contributions: Data curation, L.F.; Formal analysis, L.F. and J.X.; Funding Acquisition, J.X.; Investigation, L.F. and G.Z.; Methodology, L.F.; Project Administration, G.Z.; Resources, L.F.; Software, G.Z.; Supervision, J.X.; Validation, G.Z.; Visualization, G.Z.; Writing Original Draft, L.F.; Writing Review and Editing, L.F. All authors have read and agreed to the published version of the manuscript.

Funding: This research was funded by National Key Research and Development Program of China, grant number No. 2018YFC1506002.

Institutional Review Board Statement: Not applicable.

Informed Consent Statement: Not applicable.

Data Availability Statement: The data that support the findings of this study are available in the open literature.

Acknowledgments: We would like to acknowledge Huade Guan of Flinders University for his assistance in discussing the impact of urbanization on precipitation.

Conflicts of Interest: The authors declare no conflict of interest.

References

1. Changnon, S.A. The La Porte weather anomaly—fact or fiction? *Bull. Am. Meteorl. Soc.* **1968**, *49*, 4–11.
2. Landsberg, H.E. Man-made climate changes. *Science* **1970**, *170*, 1265–1274.
3. Huff, F.A.; Changnon, S.A. Precipitation modification by major urban areas. *Bull. Am. Meteorol. Soc.* **1973**, *54*, 1220–1232.
4. Wang, J.; Feng, J.M.; Yan, Z.W. Potential sensitivity of warm season precipitation to urbanization extents: Modeling study in Beijing-Tianjin-Hebei urban agglomeration in China. *J. Geophys. Res. Atmos.* **2015**, *120*, 9408–9425.
5. Changnon, S.A.; Semonin, R.G.; Huff, F.A. A hypothesis for urban precipitation anomalies. *J. Appl. Meteorol.* **1976**, *15*, 544–560.
6. Ochs, H.T.; Semonin, R.G. Sensitivity of a cloud microphysical model to an urban environment. *J. Appl. Meteorol.* **1979**, *18*, 1118–1129.

7. Bornstein, R.; Lin, Q. Urban heat islands and summertime convective thunderstorms in Atlanta: Three case studies. *Atmos. Environ.* **2000**, *34*, 507–516.
8. Shepherd, J.M.; Pierce, H.; Negri, A.J. Rainfall modification by major urban areas: Observations from spaceborne rain radar on the TRMM satellite. *J. Appl. Meteorol.* **2002**, *41*, 689–701.
9. Quah, A.K.L.; Roth, M. Diurnal and weekly variation of anthropogenic heat emissions in a tropical city, Singapore. *Atmos. Environ.* **2012**, *46*, 92–103.
10. Zhong, S.; Yang, X.Q. Mechanism of Urbanization Impact on a Summer Cold-Frontal Rainfall Process in the Greater Beijing Metropolitan Area. *J. Appl. Meteorol. Climatol.* **2015**, *54*, 1234–1247.
11. Niyogi, D.; Pyle, P.; Lei, M.; Arya, S.P.; Kishtawal, C.M.; Shepherd, M.; Chen, F.; Wolfe, B. Urban Modification of Thunderstorms: An Observational Storm Climatology and Model Case Study for the Indianapolis Urban Region. *J. Appl. Meteorol. Climatol.* **2011**, *50*, 1129–1144.
12. Qin, Z.; Zhang, J.E.; Luo, S.M.; Zhang, J.; Li, Y. Study on coordinative development between urbanization and eco-environment in Guangdong Province. *Ecol. Sci.* **2012**, *31*, 42–47. (In Chinese)
13. Wai, K.M.; Wang, X.M.; Lin, T.H.; Wong, M.S.; Zeng, S.K.; He, N.; Ng, E.; Lau, K.; Wang, D.H. Observational evidence of a long-term increase in precipitation due to urbanization effects and its implications for sustainable urban living. *Sci. Total Environ.* **2017**, *599*, 647–654.
14. Bolen, S.M.; Chandrasekar, V. Quantitative cross validation of space-based and ground-based radar. *J. Appl. Meteorol.* **2000**, *39*, 2071–2079.
15. Yang, Y.; Chen, X.; Qi, Y.C. Classification of convective/stratiform echoes in radar reflectivity observations using a fuzzy logic algorithm. *J. Geophys. Res. Atmos.* **2013**, *118*, 1896–1905.
16. Dou, J.J.; Wang, Y.C.; Bornstein, R.; Miao, S.G. Observed Spatial Characteristics of Beijing Urban Climate Impacts on Summer Thunderstorms. *J. Appl. Meteorol. Climatol.* **2015**, *54*, 94–105.
17. Ma, H.; Jiang, Z.; Jie, S.; Dai, A.; Fei, H. Effects of urban land-use change in East China on the East Asian summer monsoon based on the CAM5.1 model. *Clim. Dyn.* **2016**, *46*, 2977–2989.
18. Song, X.M.; Zhang, J.Y.; AghaKouchak, A.; Roy, S.S.; Xuan, Y.Q.; Wang, G.Q.; He, R.M.; Wang, X.J.; Liu, C.S. Rapid urbanization and changes in spatiotemporal characteristics of precipitation in Beijing metropolitan area. *J. Geophys. Res. Atmos.* **2014**, *119*, 11250–11271.
19. Thielen, J.; Wobrock, W.; Gadian, A.; Mestayer, P.G.; Creutin, J.D. The possible influence of urban surfaces on rainfall development: A sensitivity study in 2D in the meso-gamma-scale. *Atmos. Res.* **2000**, *54*, 15–39.
20. Zhang, N.; Gao, Z.Q.; Wang, X.M.; Chen, Y. Modeling the impact of urbanization on the local and regional climate in Yangtze River Delta, China. *Theor. Appl. Climatol.* **2010**, *102*, 331–342.
21. Wang, J.; Feng, J.M.; Yan, Z.W.; Hu, Y.H.; Jia, G.S. Nested high-resolution modeling of the impact of urbanization on regional climate in three vast urban agglomerations in China. *J. Geophys. Res. Atmos.* **2012**, *117*, D21103.
22. Liu, G.S.; Fu, Y.F. The characteristics of Tropical precipitation profiles as inferred from satellite radar measurements. *J. Meteorol. Soc. Jpn.* **2001**, *79*, 131–143.
23. Kodama, Y.M.; Tamaoki, A. A re-examination of precipitation activity in the subtropics and the mid-latitudes based on satellite-derived data. *J. Meteorol. Soc. Jpn.* **2002**, *80*, 1261–1278.
24. Fu, Y.F.; Lin, Y.H.; Liu, G.S., Wang, Q. Seasonal characteristics of precipitation in 1998 over East Asia as derived from TRMM PR. *Adv. Atmos. Sci.* **2003**, *20*, 511–529.
25. Schumacher, C.; Houze, R.A. Stratiform rain in the tropics as seen by the TRMM precipitation radar. *J. Clim.* **2003**, *16*, 1739–1756.
26. Schumacher, C.; Houze, R.A.; Kraucunas, I. The tropical dynamical response to latent heating estimates derived from the TRMM precipitation radar. *J. Atmos. Sci.* **2004**, *61*, 1341–1358.
27. Schumacher, C.; Houze, R.A. Stratiform precipitation production over sub-Saharan Africa and the tropical East Atlantic as observed by TRMM. *Q. J. R. Meteorol. Soc.* **2006**, *132*, 2235–2255.
28. Yamamoto, M.K.; Furuzawa, F.A.; Higuchi, A.; Nakamura, K. Comparison of diurnal variations in precipitation systems observed by TRMM PR, TMI, and VIRS. *J. Clim.* **2008**, *21*, 4011–4028.
29. Li, W.; Chen, S.; Chen, G.; Sha, W.; Wang, B. Urbanization signatures in strong versus weak precipitation over the Pearl River Delta metropolitan regions of China. *Environ. Res. Lett.* **2011**, *6*, 034020.
30. Zhang, Y.; Smith, J.A.; Luo, L.F.; Wang, Z.F.; Baeck, M.L. Urbanization and Rainfall Variability in the Beijing Metropolitan Region. *J. Hydrometeorol.* **2014**, *15*, 2219–2235.
31. Mcleod, J.; Shepherd, M.; Konrad, C.E. Spatio-temporal rainfall patterns around Atlanta, Georgia and possible relationships to urban land cover. *Urban Clim.* **2017**, *21*, 27–42.
32. Changnon, S.A. Precipitation changes in summer caused by St. Louis. *Science* **1979**, *205*, 402–404.
33. Sanderson, M.; Gorski, R. The effect of metropolitan Detroit–Windsor on precipitation. *J. Appl. Meteorol.* **1978**, *17*, 423–427.
34. Huff, F.A.; Vogel, J.L. Urban, topographic and diurnal effects on precipitation in the St. Louis region. *J. Appl. Meteorol.* **1978**, *17*, 565–577.
35. Braham, R.R.; Dungey, M.J. A Study of Urban Effects on Radar First Echoes. *J. Appl. Meteorol.* **1978**, *17*, 644–654.
36. Dixon, P.G.; Mote, T.L. Patterns and causes of Atlanta's urban Heat Island–initiated precipitation. *J. Appl. Meteorol.* **2003**, *42*, 1273–1284.

37. Jauregui, E.; Romales, E. Urban effects on convective precipitation in Mexico City. *Atmos. Environ.* **1996**, *30*, 3383–3389.
38. Xu, Y.P.; Xu, J.T.; Ding, J.J.; Chen, Y.; Yin, Y.X.; Zhang, X.Q. Impacts of urbanization on hydrology in the Yangtze River Delta, China. *Water Sci. Technol.* **2010**, *62*, 1221–1229.
39. Craig, K.J. MM5 simulations of urban-induced convective precipitation over Atlanta, Georgia. *Dr. Diss. San Jose State Univ.* **2002**, doi:10.31979/etd.7tgr-84sm.
40. Van Den Heever, S.C.; Cotton, W.R. Urban aerosol impacts on downwind convective storms. *J. Appl. Meteorol. Climatol.* **2007**, *46*, 828–850.
41. Hjelmfelt, M.R. Numerical simulation of the effects of St. Louis on mesoscale boundary-layer airflow and vertical air motion: Simulations of urban vs non-urban effects. *J. Appl. Meteorol.* **1982**, *21*, 1239–1257.
42. Shepherd, J.M.; Carter, M.; Manyin, M.; Messen, D.; Burian, S. The impact of urbanization on current and future coastal precipitation: A case study for Houston. *Environ. Plan. B Plan. Des.* **2010**, *37*, 284–304.
43. Lin, C.Y.; Chen, W.C.; Liu, S.C.; Liou, Y.A.; Liu, G.R.; Lin, T.H. Numerical study of the impact of urbanization on the precipitation over taiwan. *Atmos. Environ.* **2008**, *42*, 2934–2947.
44. Zhong, S.; Yun, Q.; Zhao, C.; Leung, R.; Liu, D. Urbanization-induced urban heat island and aerosol effects on climate extremes in the Yangtze river delta region of china. *Atmos. Chem. Phys.* **2017**, *17*, 5439–5457.
45. Simmonds, I.; Kaval, J. Day-of-the week variation of precipitation and maximum temperature in Melbourne, Australia. *Arch. Meteorol. Geophys. Bioclimatol. Ser. B Theor. Appl. Climatol.* **1986**, *36*, 317–330.
46. Kaufmann, R.K.; Seto, K.C.; Schneider, A.; Liu, Z.; Zhou, L.; Wang, W. Climate response to rapid urban growth: Evidence of a human-induced precipitation deficit. *J. Clim.* **2007**, *20*, 2299–2306.
47. Changnon, S.A. Urban modification of freezing-rain events. *J. Appl. Meteorol.* **2003**, *42*, 863–870.
48. Givati, A.; Rosenfeld, D. Quantifying precipitation suppression due to air pollution. *J. Appl. Meteorol.* **2004**, *43*, 1038–1056.
49. Guo, X.; Fu, D.; Wang, J. Mesoscale convective precipitation system modified by urbanization in Beijing City. *Atmos. Res.* **2006**, *82*, 112–126.
50. Zhang, C.L.; Chen, F.; Miao, S.G.; Li, Q.C.; Xia, X.A.; Xuan, C.Y. Impacts of urban expansion and future green planting on summer precipitation in the Beijing metropolitan area. *J. Geophys. Res. Atmos.* **2009**, *114*, D02116.
51. Wang, J.; Feng, J.M.; Yan, Z.W. Impact of Extensive Urbanization on Summertime Rainfall in the Beijing Region and the Role of Local Precipitation Recycling. *J. Geophys. Res. Atmos.* **2018**, *123*, 3323–3340.
52. Rosenfeld, D.; Dai, J.; Yu, X.; Yao, Z.; Xu, X.; Yang, X.; Du, C. Inverse relations between amounts of air pollution and orographic precipitation. *Science* **2007**, *315*, 1396–1398.
53. Liu, Y.; Xiao, J.; Ju, W.; Liu, Y.; Xiao, J.; Ju, W.; Xu, K.; Zhao, Y. Recent trends in vegetation greenness in China significantly altered annual evapotranspiration and water yield. *Environ. Res. Lett.* **2016**, *11*, 094010.
54. Xiao, J.F.; Moody, A. Trends in vegetation activity and their climatic correlates: China 1982 to 1998. *Int. J. Remote Sens.* **2004**, *25*, 5669–5689.
55. Park, H.S.; Sohn, B.J. Recent trends in changes of vegetation over East Asia coupled with temperature and rainfall variations. *J. Geophys. Res. Atmos.* **2010**, *115*, D14101.
56. Chen, B.; Xu, G.; Coops, N.C.; Ciais, P.; Innes, J.L.; Wang, G.; Myneni, R.B.; Wang, T.; Krzyzanowski, J.; Li, Q.; Cao, L. Changes in vegetation photosynthetic activity trends across the asia–pacific region over the last three decades. *Remote Sens. Environ.* **2014**, *144*, 28–41.
57. Xiao, J.F.; Zhou, Y.; Zhang, L. Contributions of natural and human factors to increases in vegetation productivity in China. *Ecosphere* **2015**, *6*, 233.
58. Bin, C.; Xiang-De, X.; Tianliang, Z. Main moisture sources affecting lower Yangtze River Basin in boreal summers during 2004-2009. *Int. J. Climatol.* **2013**, *33*, 1035–1046.
59. Li, L.; Dolman, A.J.; Xu, Z. Atmospheric Moisture Sources, Paths, and the Quantitative Importance to the Eastern Asian Monsoon Region. *J. Hydrometeorol.* **2016**, *17*, 637–649.
60. Zhou, T.J.; Yu, R.C. Atmospheric water vapor transport associated with typical anomalous summer rainfall patterns in China. *J. Geophys. Res. Atmos.* **2005**, *110*, D08104.
61. Hartmann, H.; Becker, S.; King, L. Predicting summer rainfall in the Yangtze River Basin with neural networks. *Int. J. Climatol.* **2008**, *28*, 925–936.
62. Shi, P.J.; Sun, S.; Wang, M.; Li, N.; Wang, J.A.; Jin, Y.Y.; Gu, X.T.; Yin, W.X. Climate change regionalization in China (1961–2010). *Sci. China-Earth Sci.* **2014**, *57*, 2676–2689.
63. Huff, F.A.; Changnon, S.A. Climatological assessment of urban effects on precipitation at St. Louis. *J. Appl. Meteorol.* **1972**, *11*, 823–842.
64. Hagemeyer, B.C. A lower-tropospheric thermodynamic climatology for March through September: Some implications for thunderstorm forecasting. *Weather Forecast.* **1991**, *6*, 254–270.
65. Changnon, S.A.; Shealy, R.T.; Scott, R.W. Precipitation Changes in Fall, Winter, and Spring Caused by St. Louis. *J. Appl. Meteorol.* **1991**, *30*, 126–134.
66. Ding, Y.H.; Sun, Y.; Wang, Z.Y.; Zhu, Y.X.; Song, Y.F. Inter-decadal variation of the summer precipitation in China and its association with decreasing Asian summer monsoon Part II: Possible causes. *Int. J. Climatol.* **2009**, *29*, 1926–1944.
67. Wang, F.; Yang, S. Regional characteristics of long-term changes in total and extreme precipitations over China and their links to atmospheric-oceanic features. *Int. J. Climatol.* **2017**, *37*, 751–769.

68. Yan, Z.W.; Wang, J.; Xia, J.J.; Feng, J.M. Review of recent studies of the climatic effects of urbanization in China. *Adv. Clim. Chang. Res.* **2016**, *7*, 154–168.
69. Dee De, R.P. Uppala, Simmons, Vitart. The ERA-Interim reanalysis: Configuration and performance of the data assimilation system. *Q. J. R. Meteorol. Soc.* **2011**, *137*, 553–597.
70. Chang, A.T.C.; Chiu, L.S. Nonsystematic Errors of Monthly Oceanic Rainfall Derived from SSM/I. *Mon. Weather Rev.* **2000**, *127*, 1630–1638.
71. Bell, T.L.; Kundu, P.K.; Kummerow, C.D. Sampling Errors of SSM/I and TRMM Rainfall Averages: Comparison with Error Estimates from Surface Data and a Simple Model. *J. Appl. Meteorol.* **2001**, *40*, 938–954.
72. Rajendran, K.; Nakazawa, T. Systematic Differences between TRMM 3G68 PR and TMI Rainfall Estimates and the Possible Association with Life Cycle of Convection. *Sola* **2005**, *1*, 165–168.
73. Muller, C.; Back, L.E.; O'Gorman, P.A.; Emanuel, K.A. A model for the relationship between tropical precipitation and column water vapor. *Geophys. Res. Lett.* **2009**, *36*, L16804.
74. Lo, J.; Lau, A.; Chen, F.; Fung, J.; Leung, K. Urban modification in a mesoscale model and the effects on the local circulation in the Pearl River Delta region. *J. Appl. Meteorol. Climatol.* **2007**, *46*, 457–476.